

# Psychophysiological classification and staging of mental states during meditative practice

Thilo Hinterberger<sup>1,2,\*</sup>, Tsutomu Kamei<sup>3,4</sup>  
and Harald Walach<sup>2,4</sup>

<sup>1</sup> Section of Applied Consciousness Sciences, Department of Psychosomatic Medicine, University Hospital Regensburg, Regensburg, Germany

<sup>2</sup> Samuelli Institute, European Office, Frankfurt (Oder), Germany

<sup>3</sup> Shimane Institute of Health Science, Izumo, Japan

<sup>4</sup> Institute for Transcultural Health Studies, European University Viadrina, Frankfurt (Oder), Germany

## Abstract

The study of meditation offers a perfect setting for the study of a large variety of states of consciousness. Here, we present a classification paradigm that can be used for staging of individual meditation sessions into a variety of predefined mental states. We have measured 64 channels of the electroencephalogram (EEG) plus peripheral physiological measures in 49 participants with varying experiences in meditation practice. The data recorded in a meditation session of seven meditative tasks were analyzed with respect to EEG power spectral density measures plus peripheral measures. A multiclass linear discriminant analysis classifier was trained for classification of data epochs of the seven standard tasks. The classification results were verified using random partitions of the data. As an overall result, about 83% ( $\pm 7\%$ ) of the epochs could be correctly classified to their originating task. The best classification method was then applied to individual meditation sessions, which allowed for staging of meditation states similarly to the staging possibility of sleep states. This study exemplarily demonstrates the possibility of developing an automatized staging tool that can be used for monitoring changes in the states of consciousness offline or online for training or therapeutic purpose.

**Keywords:** classification; electroencephalography; meditation; states of consciousness.

## Introduction

For most meditators, meditation is not a fixed state of mind that they enter at the beginning and leave after finishing their

\*Corresponding author: Prof. Dr. Thilo Hinterberger (PhD), Schwerpunkt Angewandte Bewusstseinswissenschaften, Abteilung für Psychosomatische Medizin, Universitätsklinikum Regensburg, Franz-Josef-Strauß-Allee 11, 93053 Regensburg, Germany  
Phone: +49 941 944 7241  
Fax: +49 941 944 7377  
E-mail: Thilo.Hinterberger@klinik.uni-regensburg.de

practice. According to our physiological data and the reports given by meditators about their perceived states during meditation, we clearly see that meditation can often be regarded as a process rather than a state. During meditation, a meditator might wander between states of open mindfulness, concentration, feelings of joy, distraction, etc. A variety of forms of meditation have been discussed in the literature of psychophysiological research [6, 11]. One approach is to distinguish the mind-set of open monitoring and focused attention [7, 11]. Several meditators focus their attention on their breath. However, there are also imaginative methods that make use of a mental focus (e.g., an image of the Buddha). There also exist exceptional meditation states comprising moments of contentless awareness, bliss, broader awareness, all-encompassing compassion and love, awareness of being present and being connected to other beings and/or a transcendent reality, as well as moments of special insight and knowledge. Several recently published, highly innovative papers, mainly originating from US-sponsored projects (by the Templeton Foundation, the Fetzer Institute, or the National Institutes of Health) have documented that such contemplative states are accompanied by a variety of discrete brain activation states without finding common and replicable patterns [4, 9, 18, 19, 21–24]. Recent studies from other groups support this finding [1–3, 20]. However, there is a huge variability and inhomogeneity among many studies [6]. Therefore, it is reasonable to study meditative states individually by aiming to find methods for separation of states.

In our approach, we aim to discriminate the physiological brain states of various meditation-related tasks that encapsulate certain states of consciousness. Additionally, these discrimination algorithms can be applied to a free meditation session leading to the possibility of staging of meditative states. An online application of the proposed approach allows for a real-time staging of a meditation process.

## Materials and methods

### Participants

In this study, data from 49 meditation practitioners with varying meditation experiences were used for offline classification analysis. Participants were aged between 22 and 65 years (mean 45 years, 16 females, 33 males). Thirty-one of 49 were highly experienced spiritual practitioners with >1000 h of meditation practice and 11 of 49 had <40 h, which we call low-experienced meditators. The meditators were inhomogeneously associated with different kinds of spiritual traditions and cultural background, such as Zen-Buddhism, Qi-Gong, Sahaja Yoga, Western contemplative methods, and spiritist or mediumistic

practitioners. Some of them practiced spiritual healing and Shamanism. The measurements were carried out at various locations, predominantly meditation centers or in participants' homes. Most of the Buddhist practitioners were Japanese or Chinese and were measured in Japan. Despite the heterogeneity of traditions, all meditators were able to carry out the meditative and non-meditative tasks reliably according to their reports.

All meditators participated voluntarily and gave their informed consent. The study was approved by the school Ethics Committee of the University of Northampton, UK, and the Ethics Committee of the University Clinic Freiburg i. Br., Germany.

### Measurement procedure

All physiological data were recorded with a 72-channel QuickAmp amplifier system (BrainProducts GmbH, Munich, Germany). Electroencephalogram (EEG) was measured using a 64-channel ANT Waveguard electrode cap (ANT B.V., Enschede, The Netherlands) with active shielding and Ag/AgCl electrodes, which were arranged according to the international 10/10 system. The system was grounded at the participants' shoulder. Data were recorded with a common average reference and filtered in a range from direct current (DC) to 70 Hz at a sampling rate of 250 Hz and 22-bit resolution. For correction of eye movement and blink artifacts, the vertical electrooculogram (EOG) was additionally recorded. Respiration was measured with a respiration belt and the skin conductance was derived from the second and third finger of the non-dominant hand. Additionally, for measuring the heart rate variability, the electrocardiogram was captured with two electrodes.

The measurements started with an initial 15 min baseline session in which participants sat in their meditation posture for 5 min with eyes open, 5 min with eyes closed, and spent 5 min on reading a text from a book or a computer screen. After a short break, a meditation session of 20–30 min duration was carried out in which they were asked to meditate in their own usual way, which differed across subjects. This individual meditation session was assumed to consist of a variety of mental states. It served as an experimental session to exemplify the staging approach reported here. Finally, 10 min of guided meditation was carried out in which the participant was asked to perform four different but well-defined meditative tasks, each of them for 2 min duration. These tasks consisted of 1) resting in a meditative state of presence; 2) resting in a state of thoughtless emptiness; 3) concentration on the “third eye,” which is the spot on the forehead between the eyebrows; and 4) concentration on the body axis. Thus, in total, seven epochs with different instructions were available from all meditators (Table 1). In the following classification analysis, those seven standardized task conditions served as the database as they were available for all 49 participants. One entire session lasted between 2.5h and 3 h.

### Data processing and feature selection

The whole data analysis was done using Matlab version 7.3 (Mathworks, Inc., Natick, MA, USA).

**Table 1** The seven standard conditions plus one individual meditation session.

|             |           |
|-------------|-----------|
| Eyes open   | Presence  |
| Eyes closed | Emptiness |
| Reading     | Third eye |
| Meditation  | Body axis |

#### 1) Preprocessing:

After detrending the DC-recorded EEG data sets, all EEG channels were corrected for eye movements using a linear correction algorithm. This algorithm detected eye blinks and movement events and used those periods for determining a correction factor for each channel. The EOG was multiplied with this factor and then subtracted from the EEG. It was found to work sufficiently in normal non-moving EEG and can also be applied in a real-time setting as we intend to do in the future. All EEG data were corrected for high-amplitude artifacts by limiting all EEG amplitudes to 10 times of their standard deviation. Further, a 1-Hz high-pass filter was applied.

#### 2) Autoadaptive calculation of individual frequency bands:

It has been shown in the literature [10] that the selection of standard frequency bands does not result in an optimal independence of the bands. Especially the alpha rhythm showed a clear variation with age [16]. Because the rhythms slow down with age, it would make sense to define the frequency band limits individually for each subject.

In our approach, an algorithm was developed that allowed for determining the individual alpha peak frequency (IAF) using the resting EEG data stream. Data from the eyes-closed condition were used for calculation of the IAF. The algorithm consisted of the following steps:

- Searching for the 1 min epoch in the eyes-closed data with the highest standard alpha band activity (8–12 Hz) in parietal-occipital areas. This epoch served as analysis epoch for the IAF.
- Extracting this epoch from unfiltered preprocessed raw data (corrected for EOG artifacts).
- Calculation of a high-resolution fast Fourier transform (FFT) over the 1 min epoch in the full frequency range from 0 to 70 Hz.
- Averaging of all spectra from parietal and occipital regions.
- Determining the individual expected age-dependent peak frequency as  $IAF_{exp} = 11.95 - \text{age} \times 0.053$ . By this formula, the expected alpha frequency for a 20-year-old subject would be 10.89 Hz while it decreases to 8.24 Hz in a 70-year-old person. This linear decrease of the alpha peak frequency with age has been described by Köpruner et al. [15, 16]. According to Aftanas and Golosheikine [2], the actual IAF can vary, so that the IAF was determined by searching for a peak in the high-resolution spectra in a range of  $IAF_{exp} \pm 2$  Hz.

Using this algorithm on 49 subjects, a valid peak frequency could be found in 47; in other words, in two of 49 subjects, the

peak frequency was  $>2$  Hz higher than estimated. However, those subjects also showed a very atypical spectrum that made the alpha peak hard to find by visual inspection of the spectrum. Here, the age typical frequency was chosen. Using the IAF, the frequency bands were determined as follows:

Delta: 1.5 Hz– $0.6 \times \text{IAF}$   
 Theta:  $0.6 \times \text{IAF}$ – $0.8 \times \text{IAF}$   
 Alpha:  $0.8 \times \text{IAF}$ – $1.2 \times \text{IAF}$   
 Beta1: 12.5 Hz–16 Hz  
 Beta2: 16.5 Hz–24 Hz  
 Gamma1: 24.5 Hz–47 Hz  
 Gamma2: 54 Hz–70 Hz

### 3) Power spectral density:

A power spectrum time series was calculated using FFT, which was applied to the windowed EEG time series that was convolved with a Nutall-window and shifted in steps of 0.5 s. A window size of 2 s was chosen for calculation of the FFT frequency coefficients up to 10 Hz while all higher frequencies were calculated using a 1 s window. The Fourier amplitudes of the 1-s windows were multiplied by the square root of 2 to make them comparable with the 2 s windowed frequency coefficients. Their squared value resulted in power spectral densities (PSDs), which then were log-transformed for statistical distributional reasons. Seven frequency bands as defined above were calculated by merging the corresponding FFT coefficients.

### 4) Lateralization:

According to Davidson et al. [8], the hemispheric asymmetry additionally may be a parameter of interest. Therefore, the PSD between left and right hemispheric areas as shown in Figure 1 were calculated and used as parameters for later classification. Eight interhemispheric areas were defined. The mean power of a right area was subtracted from the corresponding left area band power value. For further statistical analysis, the lateralization was expressed in a relative change by normalizing the difference to the mean power in both areas.

The possible features for classification comprised the PSD sets of seven spectral bands, the lateralized band power of seven bands, heart rate, vertical EOG, phasic skin conductance, and respiration amplitudes. All measures were adjusted to an analysis sampling rate of 2 per second as given by the FFT.

## Classification method

The first aim of this classification analysis was to test the separability of the seven task conditions. In principle, to apply supervised learning algorithms to the problem of the analysis of states of consciousness, specific classes are required originating from time intervals in which a meditator was asked to fulfill a well-defined meditation task. These intervals should be long enough to be separable into a number of epochs that then can serve as trials for the state classification. Such intervals with defined tasks were available for all meditators of this study according to the experimental design as mentioned above. This study contains one long enough interval of each

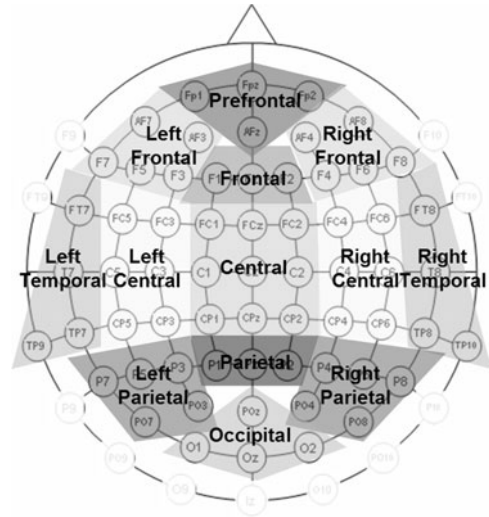


**Figure 1** The reduction scheme into eight lateralized areas is illustrated. The hemispheric lateralization values are defined by subtracting the averaged right area from the corresponding left.

of the eight conditions. Here, each 2-s-long sampling interval formed one epoch.

We focused on the question: How reliable can a classification algorithm reassociate an arbitrary short epoch of the EEG to its originating task condition? This will provide a measure for the separability of task conditions. To answer this question, the following procedure was used for a classification:

- Extraction of task sequences. The PSD of all seven standard task conditions were extracted from the three runs and concatenated to one data series. This resulted in a three-dimensional data series of size [64 channels,  $n$  samples, 7 frequency bands] and a sampling rate of 2 per second. A task vector of size  $n$  was used to specify the task condition (1...7) for each sample.
- Selection of cross-validation data. A random selection of 20% of all samples was extracted from the data series. The remaining 80% were used as training data for training of the multiclass linear discriminant analysis (LDA) classifier that was used for classification of the remaining 20%.
- Principal component analysis (PCA). The original dimension of one sample of band power data was 448 (64 channels  $\times$  7 bands). To avoid overfitting, about 10 times more samples are typically suggested for the training data set compared to the dimension of each sample vector. As a consequence, one would need about 4500 samples of training data that would require a time epoch of about 37 min for each task. Luckily, a high interdependency in the signal variation between the different electrodes is common in a 64-channel recording. Therefore, a reasonable way to reduce the channel dimension was to apply a PCA to the training data set before classification. PCA coefficients were calculated for each band separately. The PCA transformed the 64-dimensional data vector into 64 principal components that then were sorted according to the variance explained by each coefficient.

Often, already the first few coefficients explain >95% of the signal variance. Sometimes, the first component already explains >80% of the signal variance. As a good trade-off between information content and number of PCA, we chose three coefficients. This results in a training vector dimension of 21 (3 coefficients  $\times$  7 bands) meaning that <2 min of training data will be sufficient. The test data set (a 20% selection) was transformed into the same PCA coefficients by applying the transformation matrix to those data as well.

- d) Classification. For classification a multiclass Fisher's LDA [12, 17] was applied to the sample vectors. Each sample of the test data was classified into the best-fitting task condition out of the seven conditions. The best fit was defined as the smallest distance of one sample data vector to the mean training vector of a certain task condition. Several combinations of EEG measures were used to explore the contribution of different measures. For this, a variety of different classification methods were formed, which were compared in the following section.
- e) Twenty-fold 20 cross-validation. Steps 2–4 were repeated 20 times in a loop, i.e., a 20-fold 20 cross-validation process. The classification results of all 20 repetitions were averaged, resulting in a mean classification accuracy for each task condition separately. For an overall classification result, the accuracies from all seven conditions were averaged.

## Results of classification

In the process of finding an appropriate method for staging a meditation session, several sets of measures included in the data vector for classification were studied.

### Impact of individual measures

The first goal was to obtain an insight into the amount of information that is contained in the feature variables that were extracted from the EEG and also the peripheral measures with respect to the reliability for associating a sample unit to its originating task condition.

As described above, it is necessary to reduce the number of dimensions to avoid overfitting effects. Such reduction reduces the information content and thus also the classification accuracy as illustrated in Table 2. Here, different numbers of the most important PCA coefficients were used for classification of each frequency band separately. The classification results of all bands, all task conditions, and all participants were averaged. This results in an average accuracy of 62% when using all 64 coefficients, i.e., the number of channels. Using only 21 coefficients, which was the limit for the present amount of training data, this accuracy decreases to 57%, which is not much less. The chance expectancy for classifying a sample to its originating class would be  $1/7=14.3\%$  only. Using less coefficients further reduced the information content, resulting in a 40% accuracy with three PCA coefficients only, which is still significantly higher than chance.

**Table 2** Classification result from 64 channels using different numbers of PCA coefficients.

| PCA coefficients | 2    | 3    | 4    | 10   | 21   | 64   |
|------------------|------|------|------|------|------|------|
| Average accuracy | 0.37 | 0.40 | 0.43 | 0.51 | 0.57 | 0.62 |

The classification results of all participants and all frequency bands were averaged.

Second, the classification accuracies obtained with each feature variable were compared with each other. This provided an idea of the relevance or contribution of each variable to the classification result. Therefore, each feature was classified separately according to the procedure described in "Classification method." The PCA reduced the 64-channel PSD features to a four-coefficient feature vector in order to be comparable to the four-dimensional PSD lateralization values (four localizations, namely frontal, central, temporal, and parietal).

The resulting average classification accuracies for each frequency band are shown in Figure 2. The lowest impact on the classification accuracy was given by the low-frequency lateralization measures (delta, theta, and alpha bands). The highest predictability was provided by the gamma bands, especially the lateralization of the gamma2 band. This means that just by looking at the high gamma band power or lateralization amplitudes, one could associate an arbitrary sample of the whole data set to its originating task condition with a reliability of 60%. The standard deviation across subjects is around 0.1. The peripheral measures only offer one coefficient per measure of EOG, heart rate, skin conductance, and respiration. The lowest impact was given by the phasic skin conductance (average accuracy of 23%) followed by the EOG (27%) and respiration (28%). The heart rate with 37% provided the two most predictive peripheral measures.

### Empirical search for improved classification modes

**Mode 1: Classification of all-band PSD** According to the algorithm proposed in "Classification method," the 21 PCA coefficients were composed of three coefficients per band. The resulting total accuracy after averaging all participants was 66% ( $\pm 9\%$ ). This is more than the average accuracy of 57% when using single bands only.

**Mode 2: Classification of all-band PSD plus lateralization data** To increase performance by adding the lateralization features to the PSD data, a feature vector of  $3 \times 7$  PSD plus  $4 \times 7$  lateralized PSD=49 coefficients was created. This vector was reduced to 21 coefficients by a second PCA. Classification resulted in an average accuracy of 76% ( $\pm 8\%$ ), which was significantly higher than mode 1 using PSD band data only.

**Mode 3: Classification of all-band PSD, lateralization plus peripheral data** Mode 3 included as many measures as possible by using three coefficients of the 64-channel PSD of each of the seven frequency bands, four lateralized area PSD data of each of the seven frequency bands plus four

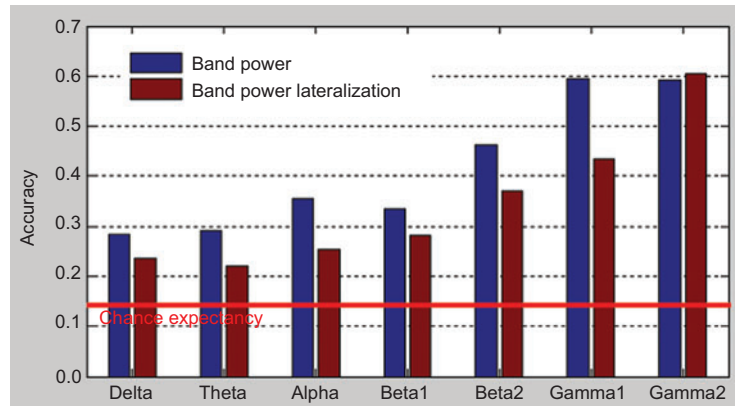


**Figure 2** Comparison in information content of band power and band power lateralization. Each bar was calculated using four coefficients for classification. Results from all participants were averaged. The standard deviation between subjects was approximately 0.10–0.12.

peripheral data. This resulted in a total of 53 coefficients per sample to be classified. This set was also reduced to the most meaningful 21 coefficients using a second PCA. This allowed for the comparability of the performance with previous modes.

Although this method included information of all frequency bands of the PSD and the lateralization PSD data, plus the peripheral data, the results decreased to 67%, i.e., roughly the same performance as mode 1. This shows that the inclusion of more measures does not necessarily lead to higher classification rates.

**Mode 4: Single-band classification of PSD** The previous results forced us to pay more attention to individual bands. The question of whether information of single bands in respect of separation of classes exceeds the use of all bands is answered in this mode. Here, the data vectors consisted of 21 PCA coefficients of the PSD from one of the seven frequency bands similarly to Table 2. While the use of 4 coefficients only resulted in a maximum of about 60% correct classification rate, the use of 21 coefficients could improve the performance in all frequency bands, resulting in an average accuracy of 79% in the high gamma band. Thus, both low and high gamma bands with 78% and 79% offer higher classification rates than using all bands and features as done in modes 1–3.

**Mode 5 (selection 1): gamma band PSD and peripheral data** The previous results asked for a more thorough selection of parameters to be used as classifier input. Adding the four peripheral data coefficients to the highest-ranking 17 coefficients high gamma PSD for obtaining a vector with 21 coefficients resulted in a further increase of the PSD to 84% at average.

**Mode 6 (selection 2): gamma band PSD and peripheral data** The gamma band lateralization offered similar high-accuracy values than the gamma band PSD. Therefore, it was attempted in mode 6 to add the gamma1 band of the lateralized data to the set. This required a reduction of the gamma2 PSD to 13 coefficients in order to obtain 21 coefficients in

total. However, the result of 83% could not exceed the previous mode.

**Mode 7 (selection 3): selection of PSD and peripheral data** After studying the results in Figure 2 by looking for the highest-ranking parameters in terms of accuracy rates and also considering the possibly most independent parameters, we came out with a subset of parameters that seemed appropriate for a sufficiently improved classification that can serve as a method for the further staging example. This set included the alpha, beta1 (SMR), beta2, and gamma2 band PSD values; the beta2 and gamma2 lateralization data; and the four peripheral measures. Again, three PCA coefficients were used for each band. The gamma 1 band seemed to be highly correlated to the gamma2 band and thus was not included. The delta and theta bands do not seem to classify very well and therefore were excluded as well. The same was true for the skin conductance and respiration measures. Altogether, 24 coefficients formed one sample vector, which was reduced to 21 coefficients for comparability with previous modes. Over all tasks, a mean classification accuracy of 83% ( $\pm 7\%$ ) could be achieved with this method. As this mode offered the lowest standard deviation across participants, it can be regarded as the most robust one.

### Summary and comparison of different classification modes

Table 3 summarizes the results of the various classification modes reported in the previous paragraph. The comparison shows that the amount of parameters included for classification is not the essential factor for obtaining an optimized classification performance. It is rather the wise selection of relevant measures that contribute to the identification of the different states. Such sets of measures have been found in modes 5–7, which succeeded the other modes. Figure 3 displays the classification accuracy of the highest ranking mode 5 for each subject separately but averaged over all task conditions. In contrast, Figure 4 illustrates the performance of mode 7 for each task condition but averaged over all participants. As mode 7 offers one of the highest classification

**Table 3** Overview of classification modes and results.

| Classification mode | Classified measures  | No. of coefficients  | Total accuracy (SD) (all participants, all tasks) |
|---------------------|--|--|---|
| 1                   | PSD (all 7 bands)  | $3 \times 7 = 21$  | 0.66 (0.09)                                       |
| 2                   | PSD and lat. PSD (all 7 bands)                                       | $3 \times 7 + 4 \times 7 = 49 \rightarrow \text{PCA} \rightarrow 21$                 | 0.76 (0.08)                                       |
| 3                   | PSD and lat. PSD (all 7 bands) and all peripheral                    | $3 \times 7 + 4 \times 7 + 4 = 53 \rightarrow \text{PCA} \rightarrow 21$             | 0.67 (0.09)                                       |
| 4                   | PSD (Delta)  | 21   | 0.38 (0.06)                                       |
| 4                   | PSD (Theta)  | 21   | 0.37 (0.06)                                       |
| 4                   | PSD (Alpha)  | 21   | 0.47 (0.08)                                       |
| 4                   | PSD (Beta1)  | 21   | 0.44 (0.09)                                       |
| 4                   | PSD (Beta2)  | 21   | 0.60 (0.10)                                       |
| 4                   | PSD (Gamma1)   | 21   | 0.78 (0.09)                                       |
| 4                   | PSD (Gamma2)   | 21   | 0.79 (0.07)                                       |
| 5 (Selection 1)     | PSD (G2) and all peripheral  | $17 + 4 = 21$  | 0.84 (0.08)                                       |
| 6 (Selection 2)     | PSD (G2), lateralized PSD (G1) and all peripheral                    | $13 + 4 + 4 = 21$  | 0.83 (0.08)                                       |
| 7 (Selection 3)     | PSD (A, B1, B2, G2), lateralized PSD (B2, G2),<br>and all peripheral | $3 \times 4 + 4 \times 2 + 4 = 24 \rightarrow 2^{\text{nd}}$<br>PCA $\rightarrow 21$ | 0.83 (0.07)                                       |

All PCA transformations on 64-channel PSD data resulted in a reduction to three coefficients; band names are D, Delta; T, Theta; A, Alpha; B1, Beta1=SMR; B2, Beta2; G1, Gamma1; G2, Gamma2; S, signal shifts; 49 participants were averaged; seven standard task conditions were averaged.

accuracies and the lowest standard deviation, this mode offers the most robust and reliable set of variables and we decided to use it for the following part of our studies, i.e., the demonstration of a staging process.

## Continuous data stream classification

### Classification within a meditation session

For a continuous data stream classification, it is necessary to have training data available defining a number of specific states of consciousness. In our study, the meditation sessions have been classified into the seven standardized tasks. That means that for classification of the freestyle meditation session, seven standard task conditions (i.e., the initial three baseline recording tasks and the four guided meditation tasks) served as training data sets for

the multiclass LDA classifier. The classification process was carried out on the meditation data sample by sample, determining the distance of the sample data vector to each of the seven classes. The class with the nearest distance was defined as the classification result. Figure 5 shows the distribution of the amount of data samples from the meditation session that has been classified to one of the seven remaining tasks for each participant separately. There is a huge variability between subjects, but for almost all subjects one can see that their EEG during meditation was from time to time similar to different tasks.

### Staging of states of consciousness

This method can be used for continuous data stream classification as well. For testing this procedure, a graphic display method was scripted that illustrates the classification results

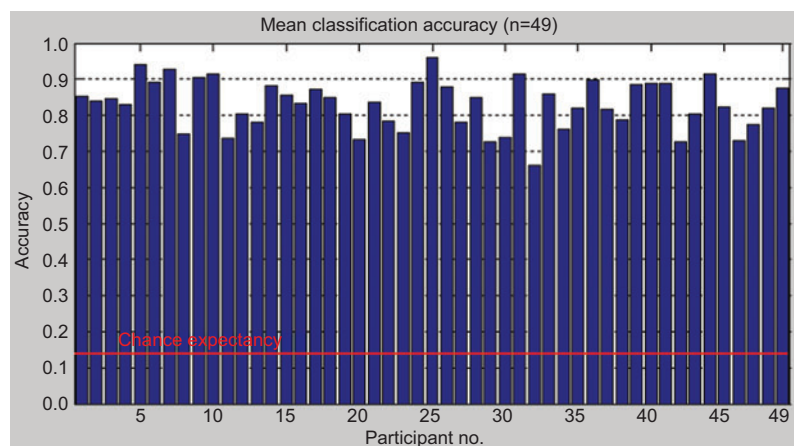


**Figure 3** Individual classification results for all 49 subjects calculated with mode 7. The total correct response rate for all task conditions is displayed after averaging the results of all task conditions. Again, in random data sets, 14.3% would be the chance expectation.

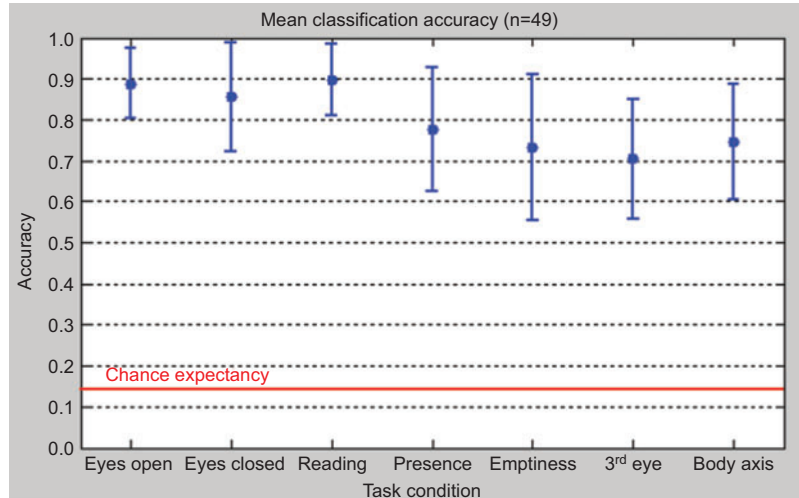


**Figure 4** The mean classification accuracy of mode 7 is depicted for each task separately. Forty-nine meditators of various experiences were averaged. The error bars are the standard deviations between meditators. Again, 14.3% would be the chance expectation in random data sets.

over time using mode 7. Such a graph can be regarded as a kind of a staging diagram of states of consciousness, similarly to the staging of sleep stages. Although the seven standard tasks cannot be ordered linearly into states of meditation depth, it seems to make sense to order them in terms of their “exceptionality” of a state of consciousness due to the task condition. Therefore, the most common and non-meditative state was associated with the reading condition and was displayed at the top row. Below that, the resting states with eyes open and then with eyes closed were listed.

All states below the second row thus were eyes-closed states. The eyes-closed condition was followed by the meditative presence, then the concentrative condition on the third eye and on the energy of the body axis. The deepest state displayed at the bottom line was the state of emptiness. For each point in time, the classification result was marked with a dot in the corresponding row. The results are staging diagrams as shown in Figure 6. As we have shown above, the states could be correctly recognized to an extent of about 70–90%; thus, it can be assumed that the staging as shown

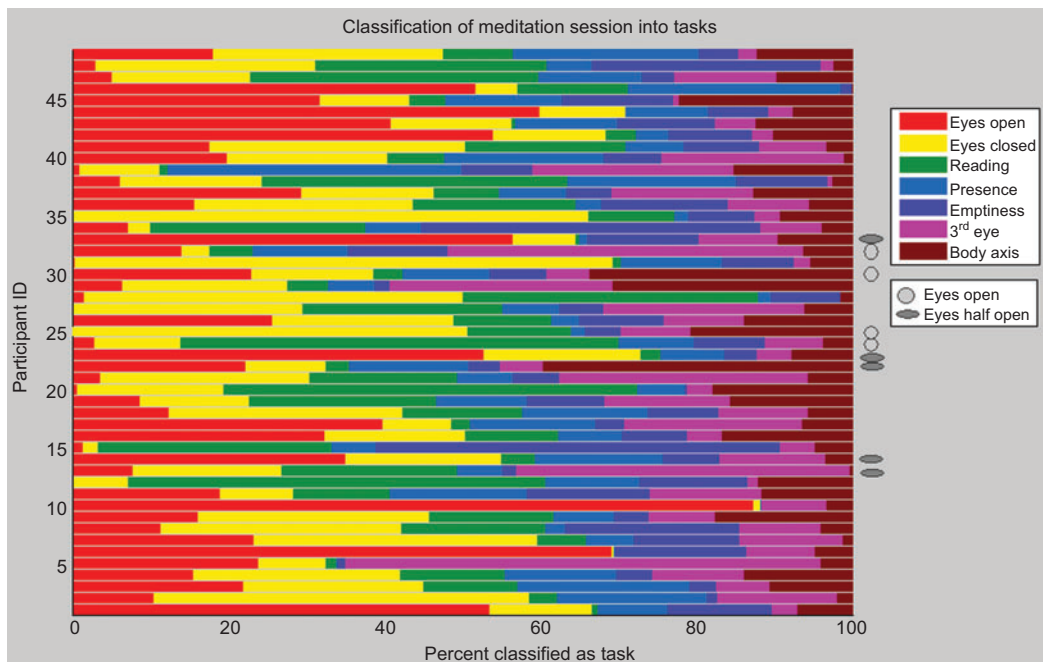


**Figure 5** Individual amount of classification results within the meditation session for all 49 subjects. The gray circles and ovals mark those meditators who had their eyes open or half open during the meditation session.

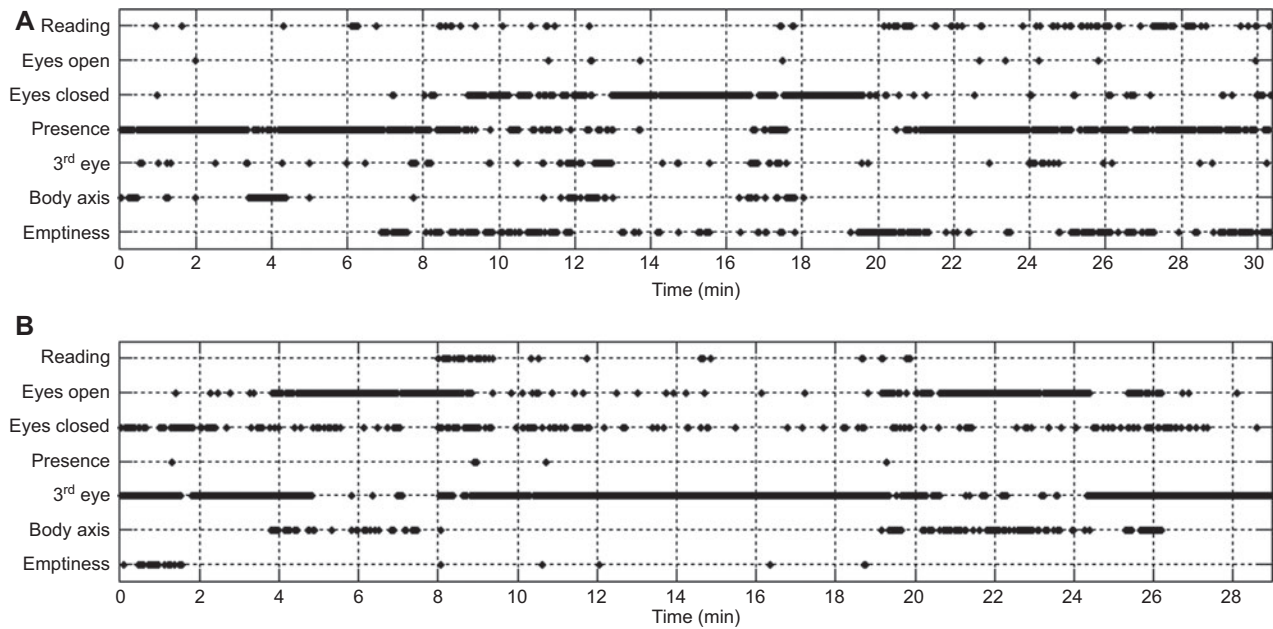


**Figure 6** Exemplary staging diagrams of states of consciousness are shown during a free and unguided meditation session without predefined tasks of two different meditators in (A) and (B). For classification of this staging example, EEG data and peripheral measures were included according to mode 7.

in the figure is highly reliable as well. While the meditator in a) remained in a state of presence during the first and last third, and the middle part was most similar to the eyes-closed condition, the meditator in b) often stayed in a state most similar to the concentration on the third eye.

## Discussion

In the section “Results of classification,” we show that, in general, samples from the EEG and physiological measures recorded during different meditative and non-meditative tasks could be reassociated to their task condition with 83% accuracy. This goal was achieved by focusing on three problems: 1) data preprocessing and selection of variables, 2) reduction of dimensionality, and 3) data classification. The latter was performed using a standard linear multiclass discriminant analysis. The reduction of dimensionality was necessary to avoid problems of overfitting, i.e., the number of training data sets should be much larger than the number of data dimensionality. The PCA can be regarded as a common method for reduction of data dimensionality on the basis of the variance. The preprocessing of EEG data followed a standard approach as well applying artifact reduction and filtering into spectral bands using Fourier transform. The non-straightforward part in this approach was the choice of EEG and other physiological data to be included into the classification process. Through a lengthy statistical analysis procedure, we have identified a set of parameters leading to useful classification results.

As we have used all our participants for this, one might ask how well those findings generalize to another group of

people carrying out the same tasks. Looking on the relatively small variance of classification accuracy between subjects, we could have also found this selection with only a subset of participants. In other words, it is likely to achieve a similar performance using the same method on other participants in the future (meditators or non-meditators) using the same variable selection.

Despite gaining high classification accuracies, this study suffers from one potential problem – the temporal structure of the experiment in which each task only was performed once for a longer period. A more robust design against possible sequence effects would have been the repetition of all seven task conditions for several times in a randomized order. However, this may have induced other problems to the meditative tasks because, sometimes, meditators require a certain time to tune into a meditation task.

## Conclusion

Assuming the reassociation of temporal recording windows to specific tasks with about 70–90% accuracy, as shown in the section “Results of classification,” is a reliable approach, we could also assume that the association of a free meditation task to other meditative tasks as done in the section “Continuous data stream classification” is a reliable procedure as well. One might question whether the seven remaining tasks were a good choice for the so-called staging references, and we could imagine more appropriate tasks or states of consciousness, but with those data we could for the first time present an approach for realizing a quite reliable staging paradigm for altered states of consciousness.



This encouraged us to implement all signal processing and classification algorithms used here in the brain-computer interface Thought Translation Device, which we have to our disposal [5, 13, 25], that would allow for real-time staging. Here, real-time classification using a support vector machine would be available as well [14, 26]. In the future, such real-time brain-state staging could not only assist a meditator during a meditation session by receiving appropriate feedback but will also help researchers to learn online about states and their subjectively experienced correlates.

## Acknowledgments

We are grateful to all spiritual practitioners who participated in this study and who devoted their time and effort with or without reimbursement. We also thank Amanda Feilding and the Beckley Foundation for their support. This work has been supported by the BIAL Foundation (Portugal), the Beckley Foundation (UK), the Samueli Institute for Information Biology (SIIB, USA), and the US Army Medical Research and Materiel Command under Award No. W81XWH-06-1-0279 P00002. The views, opinions and/or findings contained in this report are those of the authors and should not be construed as an official Department of Defense (DoD) position, policy, or decision unless so designated by other documentation. In the conduct of research where humans are the subjects, the investigators adhered to the policies regarding the protection of human subjects as prescribed by the United States Code of Federal Regulations Title 45, Volume 1, Part 46; Title 32, Chapter 1, Part 219; and Title 21, Chapter 1, Part 50 (Protection of Human Subjects).

## Appendix

In the following, the essential part of the classification routine is drafted. The code was written in Matlab.

```
% Definitions
el=64; %64 electrodes
bandSelection=[3,4,5,6,7]; % selection of 5 spectral EEG bands
bands=5;
bandLatSelection=[5,6,7]; % selection of 3 spectral lateralized EEG bands
testPercent=20; % choose 20% of data samples for testing the classifier and 80% for training the classifier
numXValidation=20; % number of cross validation cycles
numCoeff=3; % number of PCA coefficients in first PCA
numCoeff2=21; % number of coefficients in second PCA
% do cross validation and classification with all participants
for vpi=1:vpn % go through all vpn=49 subjects
[movStd, periStd, latStd, indexStd]=ConcatStdCondBands(Preprocess_data(vpi), bandSelection, bandLatSelection);
% this function creates the data sets used for later classification, all tasks are concatenated to one array
% index(samps) is task index (1..7) of each sample, samps is total number of samples (2 per second)
% the spectral EEG data set is movStd(samps, 5bands, 64 electrodes),
```

```
% the peripheral data are periStd(samps,4),
% the lateralized EEG data are latStd(samps,3 bands,4 areas),
for xi=1:numXValidation % 20 fold cross validation
% separate the data sets randomly into training data and classification test data
[movStd_train, periStd_train, latStd_train, indexStd_train, movStd_test, periStd_test, latStd_test, indexStd_test]=SelectXValidation(movStd, periStd, latStd, indexStd, testPercent);
%movStd_train(trainsamps,5bands, 64 electrodes)... trainsamps contains 80% of samps
[mov_pca_train, mov_pca_test]=PCA(movStd_train, movStd_test, numCoeff); % first PCA only on 64 electrodes EEG data
% mov_pca_train(trainsamps, 5 bands×3 coefficients)
% append lateralized data and peripheral data and create a data matrix mov_pca_train(trainsamps,5×3+3×4+4)
...
% reduce coefficients with a second PCA
[mov_pca2_train, mov_pca2_test]=PCA(mov_pca_train, mov_pca_test, numCoeff2);
% resulting in mov_pca2_train(trainsamps,21), mov_pca2_test(testsamps,21)
class=classify(mov_pca2_test, mov_pca2_train, indexStd_train);% classification
% calculation of correct response rate
correct_tot=sum((class==indexStd_test),1)./size(class,1);
end
% average correct response rate over numXValidation
...
end
```

## References

- [1] Aftanas L, Golosheikine S. Human anterior and frontal midline theta and lower alpha reflect emotionally positive state and internalized attention: high-resolution EEG investigation of meditation. *Neurosci Lett* 2001; 310: 57–60.
- [2] Aftanas L, Golosheikine S. Non-linear dynamic complexity of the human EEG during meditation. *Neurosci Lett* 2002; 330: 143–146.
- [3] Aftanas L, Golosheikine S. Impact of regular meditation practice on EEG activity at rest and during evoked negative emotions. *Int J Neurosci* 2005; 115: 893–909.
- [4] Azari N. Neural correlates of religious experience. *Eur J Neurosci* 2001; 13: 1649–1652.
- [5] Birbaumer N, Ghanayim N, Hinterberger T, et al. A spelling device for the paralysed. *Nature* 1999; 398: 297–298.
- [6] Cahn BR, Polich J. Meditation states and traits: EEG, ERP, and neuroimaging studies. *Psychol Bull* 2006; 132: 180–211.
- [7] Davidson R. Buddha's brain: neuroplasticity and meditation. *IEEE Signal Process Mag* 2008; 25: 176.
- [8] Davidson R, Kabat-Zinn J, Schumacher J, et al. Alterations in brain and immune function produced by mindfulness meditation. *Psychosom Med* 2003; 65: 564–570.

- [9] Dietrich A. Functional neuroanatomy of altered states of consciousness: the transient hypofrontality hypothesis. *Conscious Cogn* 2003; 12: 231–256.
- [10] Doppelmayr M, Klimesch W, Pachinger T, Ripper B. Individual differences in brain dynamics: important implications for the calculation of event-related band power. *Biol Cybern* 1998; 79: 49–57.
- [11] Dunn BR, Hartigan JA, Mikulas WL. Concentration and mindfulness meditations: unique forms of consciousness? *Appl Psychophysiol Biofeedback* 1999; 24: 147–165.
- [12] Fisher R. The use of multiple measurements in taxonomic problems. *Ann Eugen* 1936; 7: 179–188.
- [13] Hinterberger T, Kübler A, Kaiser J, Neuman N, Birbaumer N. A brain-computer-interface (BCI) for the locked-in: comparison of different EEG classifications for the thought translation device. *Clin Neurophysiol* 2003; 114: 416–425.
- [14] Hinterberger T, Widmann G, Lal T, et al. Voluntary brain regulation and communication with electrocorticogram signals. *Epilepsy Behav* 2008; 13: 300–306.
- [15] Klimesch W. EEG alpha and theta oscillations reflect cognitive and memory performance: a review and analysis. *Brain Res Rev* 1999; 29: 169.
- [16] Köpruner V. Quantitative EEG in normals and in patients with cerebral ischemia. *Prog Brain Res* 1984; 62: 29–50.
- [17] Krzanowski W. Principles of multivariate analysis: a user's perspective. Oxford: Clarendon Press 1988.
- [18] Lazar S. Functional brain mapping of the relaxation response and meditation. *NeuroReport* 2000; 11: 1581.
- [19] Lazar S. Meditation experience is associated with increased cortical thickness *NeuroReport* 2005; 16: 1893–1898.
- [20] Lehmann D, Faber P, Achermann P, Jeanmonod D, Gianotti L, Pizzagalli D. Brain sources of EEG gamma frequency during volitionally meditation-induced, altered states of consciousness, and experience of the self. *Psychiatr Res-Neuroimag* 2001; 108: 111–121.
- [21] Lou H. A 15O-H<sub>2</sub>O PET study of meditation and the resting state of normal consciousness. *Hum Brain Mapp* 1999; 7: 98–105.
- [22] Lutz A. Long-term meditators self-induce high-amplitude gamma synchrony during mental practice. *Proc Natl Acad Sci USA* 2004; 101: 16369–16373.
- [23] Newberg A. Cerebral blood flow during meditative prayer: preliminary findings and methodological issues. *Percept Motor Skill* 2003; 97: 625.
- [24] Newberg AB, D'Aquili EG. The neuropsychology of spiritual experience. In: Koenig HG, editor. *Handbook of religion and mental health*, vol. 1. San Diego, CA: Academic Press 1998; 75–94.
- [25] Pham M, Hinterberger T, Neuman N, et al. An auditory brain-computer interface based on the self-regulation of slow cortical potentials. *Neurorehab Neural Res* 2005; 19: 206–218.
- [26] Schröder M, Bogdan M, Rosenstiel W, Hinterberger T, Birbaumer N. Automated EEG feature selection for brain computer interfaces. In: *Proc. 1st Int. IEEE EMBS Conf. Neural Engineering (Capri Island, Italy, 20–22 March 2003)*. 2003; 626–629.

Received June 14, 2011; accepted October 26, 2011; online first November 22, 2011